# Nozzle pressure analysis of several hydrogel on extrusion-based bioprinting using computational fluid dynamics

Juan Carlos Gómez Blanco
Centro de Cirugía de Mínima Invasión Jesús Usón, jcgomez@ccmijesususon.com

Enrique Mancha Sánchez
Centro de Cirugía de Mínima Invasión Jesús Usón, emancha@ccmijesususon.com

Diego Torrejón Martín
Escuela de Ingenierías Industriales, Universidad de Extremadura, dtorrejo@alumnos.unex.es

Juan Pablo Carrasco Amador
Escuela de Ingenierías Industriales, Universidad de Extremadura, jpcarrasco@unex.es

Francisco Miguel Sánchez Margallo
Centro de Cirugía de Mínima Invasión Jesús Usón, msanchez@ccmijesususon.com

José Blas Pagador Carrasco
Centro de Cirugía de Mínima Invasión Jesús Usón, jpagador@ccmijesususon.com

## Abstract

*Extrusion bioprinting is an additive manufacturing technology with huge possibilities in the creation of engineered tissues. There are many researches about materials, cells and their interrelation. Nevertheless, there are not many researches about how the mechanics affect to cellular viability. In this way, we have done CFD simulations to check how the viscosity of materials can affect the pressure distribution in the tip of a nozzle. These results will be updated, in future works, with simulations of several materials and geometries.*

**Keywords:** Bioprinting, computational simulation, nozzle

## 1 INTRODUCTION

Additive manufacturing is a fabrication method created in the 80' and popularised nowadays under the name of 3D printing. This kind of technology works under a simple principle: the creation of an object layer by layer. It means that a certain amount of material is disposed in a defined place in each layer, the consecutive addition of layers creates an 3D object. This fabrication method allows intricate geometry which means the possibility of fabricating objects that conventional manufacturing methods cannot allow.

Bioprinting is the application of 3D printing technologies in health or biology [1], [2], [3]. This "type" of 3D printing operates under the same principle as the conventional technology with the particularization of using with cell-laden or cell-compatible materials. Materials used in bioprinting are usually 1) polymers as Polycaprolactone (PCL) or methylcellulose and 2) hydrogels as Alginate or Hyaluronic Acid (HA). In fact, any kind of material can be used for bioprinting as long as they are biocompatible (allow cells to live and proliferate) and biodegradable [4], [5], [6]. Many previous works analyse which material is better according to the biological material to be bioprinted [7], [8], [9]. In this sense, a proper selection of the biological material is another key point. According to the clinical/medical application different stem cells are used, such as Bone Narrow Stem Cells (BNSCs) in bone scaffolds or Mesenchymal Stem Cells (MSCs) in cartilage regeneration. Cells are very sensitive and need a proper environment and nutrients to live and proliferate [10]. For this reason, a bioprinter must control, at least, temperature, pressure, $CO_2$ and pH [11].

Although other deposition methods are possible, maybe the most common techniques used in bioprinting are extrusion, inkjet and laser-assisted [12]. Mainly due to cost-effective reasons, the most used technique is the extrusion-based that deposit biomaterials through a customized nozzle [13]. So, these kinds of bioprinters use extrusion heads that are usually formed by a syringe and

a needle or a conical tip. It is well described in bibliography that the pressure is one of the most important factors that can provoke a low cell survival [8].

Computational simulations are widely extended in calculation of flows through nozzles [14], [15]. However, bioprinting related simulations have still room for improvement with only a few research studies [16], [17]. For this reason, Computational Fluids Dynamics (CFD) in bioprinting technology could provide useful data of material flows and help to select the most appropriate hydrogel for the survival of cells.

Hence, the main objective of this work is to analyse the pressure in the nozzle tip through computational fluid simulation for different biocompatible materials.

## 2 METHODS

### 2.1 MODEL

The model was designed and simulated in COMSOL Multiphysics through a 2D axisymmetric model and the Two-Phase Flow (TPF) level set interface. The model consists of two different geometries. One is the related to the nozzle, modelled by a trapezium of 25 mm of height, 3 mm of the inlet face and 0.2 mm of the outlet face. The rest of the geometry is composed by a rectangle and a trapezium which is related to the air where the nozzle ejects the material.

### 2.2 GOVERNING EQUATIONS

Level set (LS) method is a transport equation which is added to incompressible Navier-Stokes equations to track the interface of two immiscible fluids, in this case bioprinting materials and air, these equations are:

$$\rho\frac{\partial u}{\partial t} + \rho(u \cdot \nabla)u =$$
$$\nabla \cdot [-pI + \mu(\nabla u + \nabla u^T)] + F + \rho g \quad (1)$$

$$\nabla \cdot u = 0 \quad (2)$$

where, $\rho$ is the density, $u$ is the speed of the fluid, $p$ denotes the pressure, $I$ is the identity matrix, $F$ is all other external forces and $g$ is the gravity force.

In the level set equation, the bioprinting material is expressed by $\phi = 0$, the air is expressed by $\phi = 1$ and the contour lines of level set is expressed by $\phi = 0.5$. The level set equation can be seen as the volume percentage of water in the gas-liquid two-phase flow [18]. Therefore, the migration equation of the gas-liquid interface can be written as follows:

$$\frac{\partial \phi}{\partial t} + u \cdot \nabla \phi =$$
$$\gamma \nabla \left( \epsilon_{ls}\nabla\phi + \phi(1-\phi)\frac{\nabla\phi}{\nabla\phi} \right) \quad (3)$$

where $\phi$ is the contour line of the interface of the gas-liquid two-phase flow, $\gamma$ is the reinitialization parameter to solve the equation, $\epsilon$ is the interface thickness controlling parameter. The physical property parameters need to be processed smoothly to avoid the instability of the numerical calculation. These parameters are the density and viscosity of the fluid near the interface. The smoothing process of the level set equation involves the level set function to express the change in the density and viscosity of fluid during the process of the gas-liquid two-phase flow and are defined as:

$$\rho = \rho_1 + (\rho_2 - \rho_1)\phi \quad (4)$$

and the dynamic viscosity is given by:

$$\mu = \mu_1 + (\mu_2 - \mu_1)\phi \quad (5)$$

where $\rho_1$ and $\rho_2$ are the constant densities of bioprinting materials and air, respectively, and $\mu_1$ and $\mu_2$ are the dynamic viscosities of bioprinting materials and air, respectively. Here, bioprinting material corresponds to the domain where $\phi < 0.5$, and air corresponds to the domain where $\phi > 0.5$.

### 2.3 DOMAINS

In this model, two different domains were considered. The first domain is related to the nozzle and the second domain is the outside of the nozzle, the air where the biological material is ejected. Two different bioprinting hydrogels are going to be simulated. Viscosity and density of Material 1 is 0.83 $Pa \cdot s$ and 1455.08 $kg/m^3$ and Material 2 is 1.41 $Pa \; cdots$ and 1231.34 $kg/m^3$, respectively. To make possible a flow, an inlet was placed in the top part of the nozzle with a value of 1 $mm/s$.

Also, an outlet condition was set at the top part of the air domain to allow bioprinting materials to fill this domain and air to leave. An initial interface boundary condition was placed at the end of the nozzle to define a boundary where the fluid finishes and the air starts. All geometry and boundary conditions can be seen in the Figure 1.
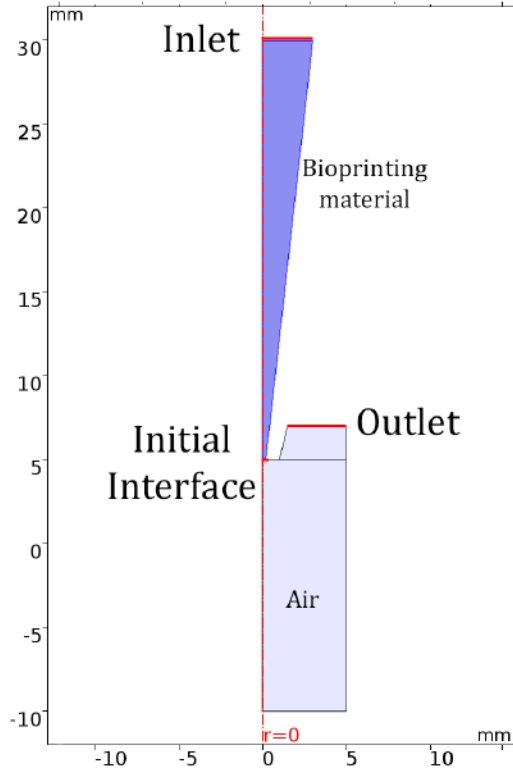


Figure 1: Representation of the geometry used in the simulations.

## 2.4 MESH

A 2D triangular mesh was created for the simulations. For better simulations an adaptive mesh refinement was set as can be seen in Figure 2. This creates multiple meshes for segments of the time-dependent simulation. Initial triangular mesh has 2892 triangular elements, while the remeshing raise the number of elements in the zone where the interface between both materials is placed as shown in Table 1.

Table 1: Mesh refinement elements and quality

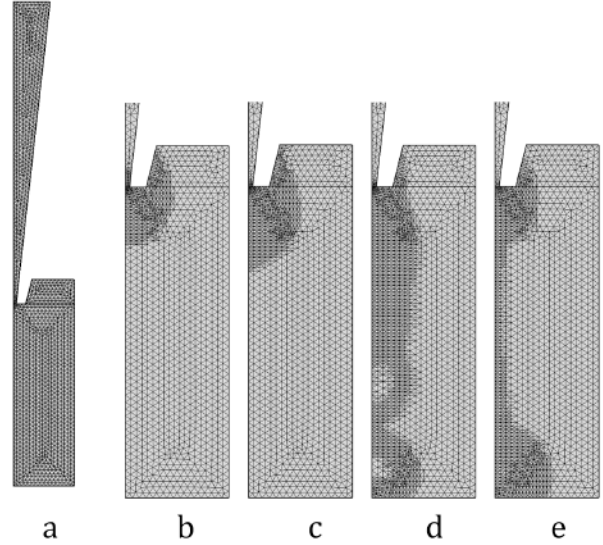| Mesh | No. of elements | Quality |
|------|-----------------|---------|
| a | 2892 | 0.9214 |
| b | 3604 | 0.8581 |
| c | 3828 | 0.8442 |
| d | 5102 | 0.7865 |
| e | 4460 | 0.8075 |



Figure 2: Original mesh (left) and mesh refinement procedure during simulations.

## 2.5 SIMULATION

Two 1.5 s simulations, with a 5 ms step, were done, one for each material. For each one of them, two study steps were created, Phase Initialization and Time Dependent. The Phase Initialization step solves for the distance to the initial interface $>$, $D_{wi}$. The Time Dependent step then uses the initial condition for the level set function according to the following expression:

$$\phi_0 = \frac{1}{1 + e^{D_{wi}/\epsilon}} \quad (6)$$

in domains initially filled with bioprinting materials and:

$$\phi_0 = \frac{1}{1 + e^{-D_{wi}/\epsilon}} \quad (7)$$

in domains initially filled with air.

## 3 RESULTS AND DISCUSSION

### 3.1 FLUID VOLUMETRIC FRACTION

The amount of each material is represented by the fluid volumetric fraction. Values 1 means that the 100% of the material is composed by a certain material (not air). Therefore 0 values mean that all the material is air. Figure 3 shows the drop formed at 0.695 $s$ of the simulation done with Material 1. The interface between the material and air is defined in the figure with a
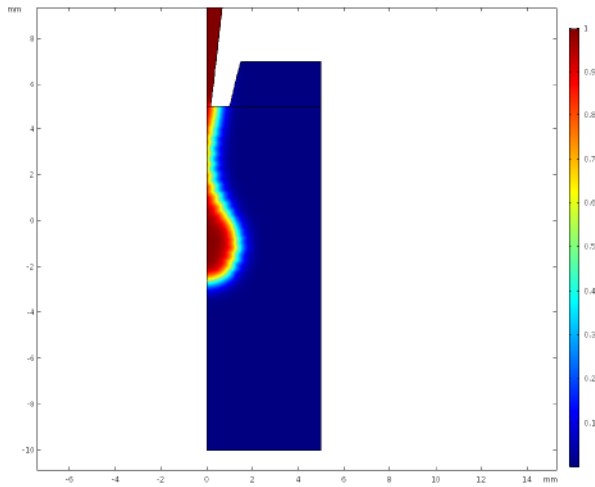
739

fluid fraction volume of 0.5.



Figure 3: Fluid Volumetric Fraction of material 1 in 0.695 s.

In the total time of Material 1 simulation ($1.5s$) two drops are formed and felt down.

Figure 4 shows the drop formed at $0.9\ s$ of the simulation done with Material 2. At the end of this simulation ($1.5s$) two drops where formed but only one of them felt down. It is clear that the viscosity of the material used have impact in drop formation time.
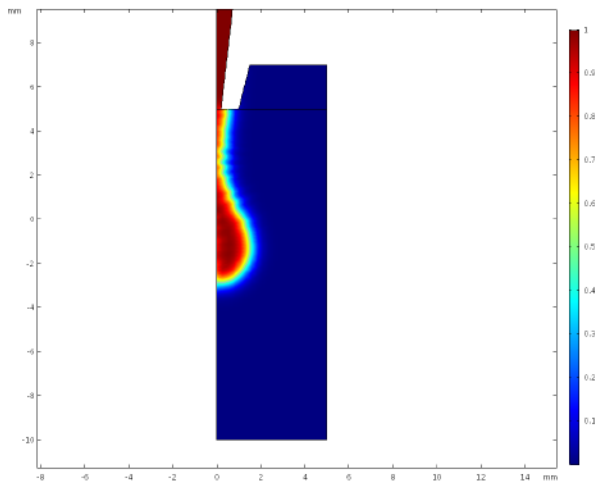


Figure 4: Fluid volumetric fraction of material 2 in 0.9 s

## 3.2  PRESSURES

Pressure plots obtained in the simulations can be seen in Figure 5 and Figure 6 for Material 1 and Material 2 respectively. Both of them have a similar shape, this fact suggests a similar pressure behaviour for the studied materials.

Pressure increases in the beginning of the drop formation, during the formation the pressure start to descend and, at last, when the drop fell there is a low-pressure peak.
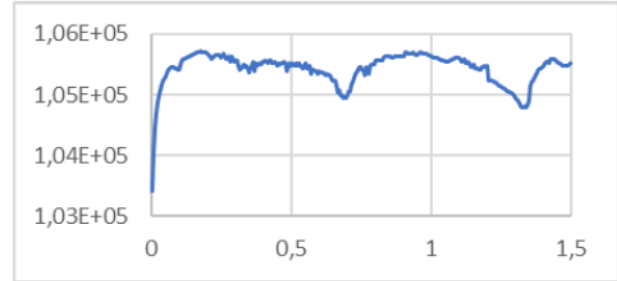


Figure 5: Material 1 pressure plot in the outlet of the nozzle.
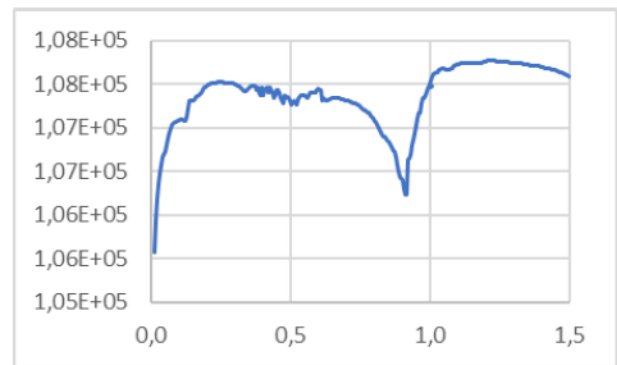


Figure 6: Material 2 pressure plot in the outlet of the nozzle.

In Material 1 there are two low-pressure peaks what means that two drops fell down. For Material 2 there is only one peak. These results correspond with the ones seen in the analysis of the Fluid Volumetric Fraction, 2 drops for Material 1 and 1 drop in Material 2.

Maximum pressure values are $1.05712 \cdot 10^5\ Pa$ and $1.07980 \cdot 10^5\ Pa$ for Material 1 and Material 2. The pressure varies for about $2 \cdot 10^4\ Pa$ comparing both materials. It can be said that the more viscosity the material is, the more pressure is needed to extrude it. However, more studies are needed for determining if the pressures reached in the simulations are in range for cellular viability.

## 4  CONCLUSIONS

In this work two different computational simulations of the flow of different materials through a nozzle have been done. We have checked that variations on the viscosity of different hydrogels provoke a variation in pressure at the nozzle tip.

740

With our results it can be said that it seems to be a tendency, the higher the viscosity the higher the pressure at the nozzle tip. However only two materials have been simulated, it is necessary further studies with a wide range of materials and viscosities to check that bias.

Hence, future simulations with modifications in nozzle tip geometry are needed to check if geometry has an important role on pressure distribution. Huge amounts of data from simulation will allow to obtain the optimum nozzle tip for each material and cell used attending to pressure distribution.

## Acknowledgement

## References

[1] H.-W. Kang, J. J. Yoo, and A. Atala, "Bioprinted Scaffolds for Cartilage Tissue Engineering," *Cartilage Tissue Engineering: Methods and Protocols*, vol. 1340, pp. 981–995, 2015.

[2] Y. D. Hesuani *et al.*, "Design and Implementation of Novel Multifunctional 3D Bioprinter," *3d Printing and Additive Manufacturing*, vol. 3, no. 1, pp. 65–68, 2016.

[3] N. Cubo *et al.*, "3D bioprinting of functional human skin: production and <i>in vivo</i> analysis," *Biofabrication*, vol. 9, no. 1, p. 015006, 2016.

[4] E. M. Ahmed, "Hydrogel: Preparation, characterization, and applications: A review," *Journal of Advanced Research*, vol. 6, no. 2, pp. 105–121, 2015.

[5] Y. He *et al.*, "Research on the printability of hydrogels in 3D bioprinting." *Scientific reports*, vol. 6, p. 29977, 2016.

[6] A. Panwar and L. P. Tan, "Current status of bioinks for micro-extrusion-based 3D bioprinting," *Molecules*, vol. 21, no. 6, 2016.

[7] J. Kim *et al.*, "Current status of three-dimensional printing inks for soft tissue regeneration," *Springer*.

[8] L. Ning and X. Chen, "A brief review of extrusion-based tissue scaffold bio-printing," *Biotechnology Journal*, vol. 12, no. 8, 2017.

[9] I. T. Ozbolat and M. Hospodiuk, "Current advances and future perspectives in extrusion-based bioprinting," *Biomaterials*, vol. 76, pp. 321–343, 2016.

[10] B. Alberts *et al.*, *Molecular Biology of the Cell*, fifth edit ed., M. Anderson and S. Granum, Eds. Garland Science, Taylor & Francis Group, LLC, 2008.

[11] Y. Zhao *et al.*, "The influence of printing parameters on cell survival rate and printability in microextrusion-based 3D cell printing technology," *Biofabrication*, vol. 7, no. 4, pp. 1–11, 2015.

[12] F. Pati *et al.*, *Extrusion bioprinting*, 2015, no. December.

[13] I. T. Ozbolat, K. K. Moncal, and H. Gudapati, "Evaluation of bioprinter technologies," *Additive Manufacturing*, vol. 13, pp. 179–200, 2017.

[14] W. Yuan and G. H. Schnerr, "Numerical Simulation of Two-Phase Flow in Injection Nozzles: Interaction of Cavitation and External Jet Formation," *Journal of Fluids Engineering*, vol. 125, no. 6, pp. 963–969, jan 2004.

[15] S. Zekovic, R. Dwivedi, and R. Kovacevic, "Numerical simulation and experimental investigation of gas–powder flow from radially symmetrical nozzles in laser-based direct metal deposition," *International Journal of Machine Tools and Manufacture*, vol. 47, no. 1, pp. 112–123, jan 2007.

[16] J. A. Reid *et al.*, "Accessible bioprinting: adaptation of a low-cost 3D-printer for precise cell placement and stem cell differentiation." *Biofabrication*, vol. 8, no. 2, p. 025017, 2016.

[17] W. Martanto *et al.*, "Fluid dynamics in conically tapered microneedles," *AIChE Journal*, vol. 51, no. 6, pp. 1599–1607, 2005.

[18] COMSOL Multiphysics, "Theory for the Two-Phase Flow Interfaces - CFD Module User's Guide," *Manual*, p. 620, 2014.